Organic Non-Nucleophilic Electrolyte Resists Carbonation During Selective CO_2 Electroreduction

An T. Chu, Onyu Jung, Wei Lun Toh, and Yogesh Surendranath*

Department of Chemistry, Massachusetts Institute of Technology, Cambridge, Massachusetts 02139, United States

Non-aqueous electrochemistry, aprotic solvent, carbon dioxide reduction, proton donor, gold, carbonate, fuels, selectivity

ABSTRACT: The spontaneous reaction of CO_2 with water and hydroxide to form (bi)carbonates in alkaline aqueous electrolytes compromises the energy and carbon-efficiency of CO_2 electrolyzers. We hypothesized that electrolyte carbonation could be mitigated in an aprotic solvent with low water content, by employing an exogenous non-nucleophilic acid capable of driving proton transfer without parasitic capture of CO_2 by its conjugate base. However, it is unclear whether such an electrolyte design could engender high CO_2 reduction selectivity and low electrolyte carbonation. We herein report selective CO_2 electroreduction on polycrystalline Au catalyst using dimethyl sulfoxide as the solvent and acetic acid / acetate as the proton donating medium with low carbonate formation. CO_2 is reduced to CO with over 90% faradaic efficiency at potentials relative to the reversible hydrogen couple that are comparable to those in neutral aqueous electrolytes. ^1H and ^{13}C NMR studies demonstrate that only millimolar concentrations of bicarbonates are reversibly formed, that the proton activity of the medium is largely unaffected by exposure to CO_2, and that low carbonation is maintained upon addition of 1 M water. This work demonstrates that electrolyte carbonation and efficient CO_2 reduction can be decoupled from each other in an aprotic solvent, offering new electrolyte design principles for low-temperature CO_2 electroreduction systems.

Introduction

Low-temperature electrochemical reduction of CO_2 (CO_2RR) is a burgeoning approach to producing value-added products from renewable energy inputs.[1,2] However, the selective production of desirable reduced carbon products is challenged by the competing hydrogen evolution reaction (HER). Mechanistic studies of transition metal cathodes such as Cu, Ag, and Au have shown that the CO_2 activation step that initiates CO_2RR is largely insensitive to the proton donor environment, whereas the HER is highly sensitive to the proton donor and pH environment. [3–6] Consequently, it has been universally observed that highly alkaline electrolytes selectively suppress HER, leading to enhanced faradaic efficiency (FE) for CO_2RR. Indeed, the high faradaic efficiency of many reported cathodes, such as nanostructured catalysts or gas diffusion electrodes,[7,8] has been attributed to their ability to engender a high interfacial pH during polarization.

While alkaline conditions foster high faradaic efficiency for CO_2RR, they compromise the carbon efficiency of CO_2 reduction. This impasse has been identified as "the carbonate problem"[9,10] and can be understood by examining the role of the proton donor (HA) with reference to a prototypical reaction stoichiometry for CO_2RR to CO (**Figure 1, top**). In alkaline aqueous environments, water is the most competent proton donor (**Figure 1a**). Its deprotonation leads to the formation of two equivalents of hydroxide, which capture CO_2 by reacting to form (bi)carbonate anions. Since (bi)carbonates are inert to direct electroreduction,[11,12] their transport across the cell leads to their release at the anode, eroding the carbon efficiency of CO_2RR at the cathode. For CO_2 reduction to CO, this process leads to a 50% carbon utilization efficiency,[9] and is even lower for more reduced products such as ethylene. At intermediate pH, bicarbonate itself can serve as the proton donor and form carbonate (**Figure 1a**). However, since CO_2 hydration generates carbonic acid, the electrogenerated carbonate dianion is subject to comproportionation to regenerate two equivalents of bicarbonate, reintroducing the carbonate problem. Indeed, the CO_2/HCO_3^- equilibrium makes electrolyte carbonation an inevitable consequence of operating at any pH above the CO_2/HCO_3^- buffer point (~pH 7).[13]

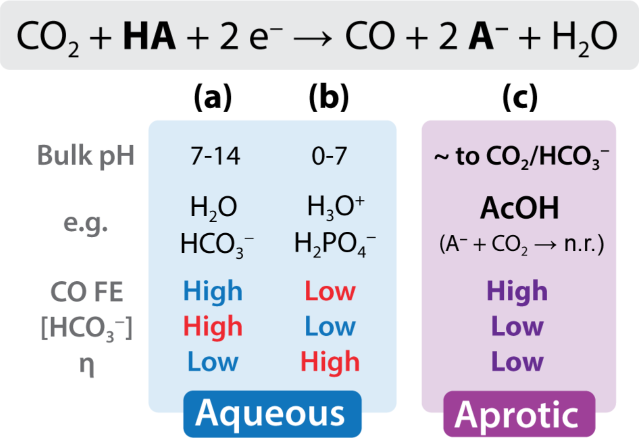

Figure 1. Schematic describing the reaction selectivity (CO FE), extent of carbonation ($[HCO_3^-]$), and overpotential (η) of CO_2RR-to-CO using proton donors (HA) of varying pK_a values and pH environments in (a,b) aqueous and (c) aprotic solvent-based electrolyte conditions.

In contrast, high carbon efficiency can be recovered by operating in an acidic electrolyte with H_3O^+ as the terminal proton donor (**Figure 1b**). Since unfettered transport of H_3O^+ to the interface would favor HER, acidic electrolytes are paired with ionomer-coatings, bipolar membranes, or high concentrations of alkali cations to foster a substantial pH gradient at the interface.[14–18] These strategies accept the formation of (bi)carbonate at the interface and attempt to reprotonate the anion elsewhere in the cell to liberate CO_2. While these approaches foster higher carbon efficiencies, they operate with a significant interfacial pH differential relative to the bulk,[14] which incurs large overpotentials in excess of 0.8 V.[18] Furthermore, the faradaic efficiency of CO_2RR is partially compromised in some designs, relative to fully alkaline electrolytes.[19] To reduce these energetic losses while avoiding carbonation, a terminal proton donor with a pK_a close to that of CO_2/HCO_3^- would be ideal but using phosphate buffers in neutral electrolytes has been shown to promote HER at the cost of CO_2RR FE. (**Figure 1b**).[12] As the foregoing discussion highlights, for aqueous CO_2RR, the proton donating environment can either be optimized for high FE and low overpotential (alkaline) at the expense of high carbon efficiency, or high carbon efficiency (acidic) at the expense of high FE and low overpotential. Thus, simultaneously achieving a high carbon efficiency, faradaic efficiency, and low overpotential faces inherent challenges in aqueous electrolytes.

We hypothesized that the above impasse could be addressed in an aprotic solvent-based electrolyte. In this media, the activity of water can be significantly suppressed, mitigating its intrinsic bias to react with CO_2 and promote PCET steps towards HER. Instead, a proton transfer agent can be chosen specifically to foster CO_2RR while inhibiting electrolyte carbonation. Indeed, CO_2RR has been demonstrated in aprotic-solvent based electrolytes: electrolysis using cathodes such as Cu or Au have been reported to engender high selectivity for C_1 products.[20] However, such designs fail to address electrolyte carbonation because trace (or exogenously added) water is utilized as the proton donor,[21–24] leading to the expected stoichiometric formation of bicarbonate as a reaction product.[25] In contrast, we envisioned that carefully selecting an exogeneous donor, with a pK_a closely matched to that of CO_2/HCO_3^-, could mitigate carbonation while maintaining high faradaic efficiency and modest overpotentials (**Figure 1c**). In addition, the selected donor must form a conjugate base that is non-nucleophilic to avoid reaction with CO_2 following PCET, eliminating a potential pathway for electrolyte-mediated CO_2 capture. When paired with electrolytes with a sufficiently low water activity, we sought to understand if selective CO_2RR could be *decoupled* from significant electrolyte carbonation in an aprotic solvent.

Herein, we report selective CO_2RR with minimal bulk carbonate formation in dimethylsulfoxide (DMSO) electrolyte utilizing acetic acid/acetate ($AcOH/AcO^-$) buffer as the proton donating medium. We selected polycrystalline Au (pc-Au) as a model catalyst to characterize the H_2/C_1 selectivity in this previously unexplored electrolyte, due to its simple CO_2RR product distribution consisting of H_2, CO and formate.[13] We demonstrate that the electrolyte medium is capable of catalyzing CO_2RR to C_1 products with over 90% faradaic efficiency with minimal H_2 formation. NMR analysis demonstrates that only millimolar concentrations of bicarbonate are formed reversibly in the electrolyte, and that attenuated electrolyte carbonation and the high C_1 reaction selectivity are maintained in electrolytes with 1 M of added water. Our results challenge the notion that carbonation is an inevitable outcome of CO_2RR, and provide a conceptual framework for enabling low-carbonate CO_2RR electrolysis towards value-added products.

Results & Discussion

Au-catalyzed CO_2 reduction in DMSO/AcOH buffer selects for C_1 products

To examine the H_2 versus C_1 product selectivity of CO_2RR, we polarized pc-Au electrodes under a CO_2 atmosphere in this previously unexplored electrolyte media. DMSO was selected for its electrochemical stability under highly reducing potentials. AcOH was selected because its carboxylate conjugate base is relatively non-nucleophilic and, as described later, possesses a similar pK_a to the CO_2/HCO_3^- equilibrium. Galvanostatic electrolyses were conducted in DMSO electrolyte (DMSO/AcOH) consisting of an analytical concentration of 0.3 M AcOH/tetrabutylammonium acetate (TBAAcO) in a 1:1 ratio with 0.15 M tetrabutylammonium hexafluorophosphate ($TBAPF_6$) supporting electrolyte. Gaseous products formed during polarization were characterized using in-line gas chromatography (see SI section 1.2 for experimental details). As discussed later, galvanostatic electrolysis were also conducted with DMSO/AcOH with 1 M of added water, henceforth referred to as "wet DMSO/AcOH". However, we stress that DMSO/AcOH was not rigorously dried and estimate an adventitious water concentration of 9 ± 2 mM (see SI section 1.3 for details). In either condition, the applied potentials for steady-state electrolysis are far removed from the solvent reduction window of the respective electrolytes without $AcOH/AcO^-$ and CO_2, confirming the reductive stability of DMSO (Figure S6). For the product selectivity studies reported in this section, a pc-Au counter electrode was utilized as the anode to avoid the possible effect of parasitic anode dissolution and contamination on the cathode reaction. However, we separately demonstrate that hydrogen oxidation can be sustained as a anode reaction using a Pt counter electrode to avoid the anodic decomposition of acetate to form carbon dioxide and ethane (i.e. Kolbe electrolysis), which has been previously reported to occur on Pt and Au anodes (see SI section 2.1 for further discussion).[26]

CO_2 electroreduction occurs with a high selectivity for C_1 products and minimal formation of H_2 in DMSO/AcOH. **Figure 2a** depicts the potential-dependent faradaic efficiency of H_2 and CO versus the cobaltocene/cobaltocenium (Cc/Cc^+) reference couple, while **Figure S7** depicts that of the faradaic balance in DMSO/AcOH (see **Figure S9** for partial current density trends per product). The selectivity for CO rises to a maximal value of ca. 90% towards −0.83 V vs Cc/Cc^+ applied potential, while H_2 is not observed across all potentials examined. CO production was ascribed to the electroreduction of CO_2, rather than parasitic decomposition of the electrolyte, based on mass spectroscopic analysis of the effluent gas stream following polarization in the presence of $^{13}CO_2$ (see SI section 2.2 for experimental details). To characterize the chemical identity of the solution-phase product(s) comprising the faradaic balance, the catholyte was sampled via ^1H NMR following constant current electrolysis in the presence of $^{13}CO_2$ (see SI section 1.5 for details). A doublet centered at 8.54 ppm was observed, characteristic of ^{13}C-formate (**Figure S7b**), indicating that formate production also originates from the reduction of CO_2. We stress that careful analysis of the potential-dependent formate production selectivity and rates is challenged by the low molar quantities produced and herein avoid its detailed interpretation. However, no other electrogenerated products were detected via ^1H or ^{13}C NMR, suggesting the complete suppression of HER in favor of C_1 product formation.

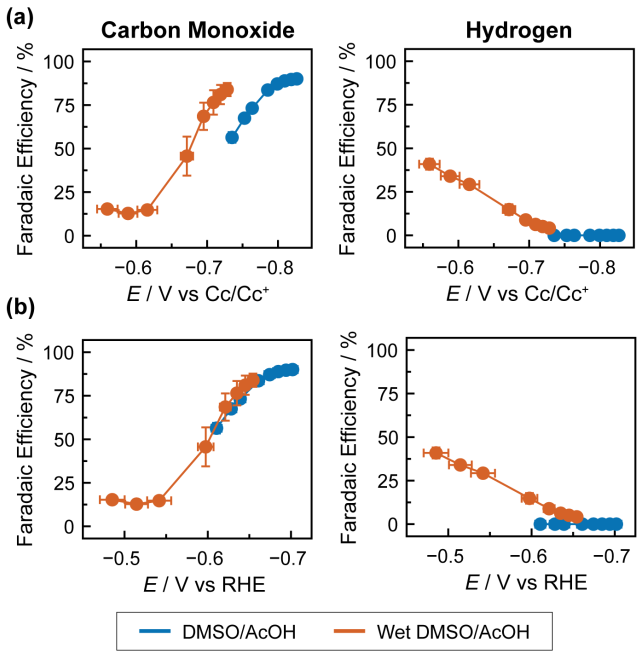

Figure 2. Potential-dependent faradaic efficiency trends for CO and H_2 in DMSO/AcOH (blue) and DMSO/AcOH with 1 M added water ("wet DMSO/AcOH", orange) electrolyte versus the (a) cobaltocene/cobaltocenium (Cc/Cc^+) internal reference potential and (b) RHE (reversible hydrogen electrode) reference potential. Electrolysis was conducted via galvanostatic polarization from −0.17 to −2.03 mA cm^{-2} on pc-Au catalyst. All current densities are normalized with respect to the electrochemically active surface area. The data points and error bars correspond to the average and standard deviation of three measurements.

To meaningfully compare CO_2RR selectivities in aqueous electrolytes and the DMSO/AcOH system at comparable applied potentials, the proton activity of each system must be determined. In water, the proton activity of the electrolyte is described by the pH, which can be easily calculated from the acid-base dissociation constant of the proton donor. This value can then be used to reference the data to the reversible hydrogen electrode (RHE) scale. In an aprotic solvent, however, the analytical determination of the proton activity is complicated by the presence of multiple solution non-idealities, such as homoconjugation and ion pairing,[27] whose complex equilibria are not conveniently characterized. To circumvent this issue, the proton activity of the system can instead be empirically determined from the equilibrium potential of the H^+/H_2 redox couple on Pt electrodes, which is directly sensitive to the activity ratio of the donor (a_{HA}) to conjugate base ($a_{\mathrm{A^-}}$).[28,29] The measured equilibrium potential can then be used to reference the applied potentials depicted in **Figure 2a** to the RHE scale, permitting an approximate comparison between the aqueous and aprotic system.

Applying this analysis demonstrates the similarity of the reaction selectivity in DMSO/AcOH compared to those in water. **Figure 2b** shows the faradaic efficiency trends of CO and H_2 referenced to the measured equilibrium potential of the H^+/H_2 redox couple (i.e. RHE; see SI section 1.8 for experimental details; see **Figure S7** and **S9** for the equivalent plots for formate). The potential-dependent CO selectivity profiles are comparable to those in aqueous buffered pH 6.8 $KHCO_3$ electrolyte at similar potentials versus RHE on pc-Au. For example, at ca. −0.7 V vs RHE, the CO selectivity is 98% in the aqueous electrolyte, while it is 90% in DMSO/AcOH.[30] In addition, the overpotentials required to achieve selective CO formation in DMSO/AcOH are less than those in acidic aqueous electrolytes. For example, in pH 1 H_2SO_4 electrolyte with 0.4 M K_2SO_4 with a Au/C catalyst,[18] polarization at −0.7 V vs RHE is completely selective for H_2, in contrast to the 90% selectivity observed for CO production in DMSO/AcOH. Achieving comparable selectivity in acidic aqueous media requires an applied potential of −1.0 V vs RHE, where the additional 0.3 V of applied overpotential is required to sustain a high interfacial pH gradient. Together, the foregoing data demonstrate that DMSO/AcOH electrolyte is not only capable of supporting selective electroreduction of CO_2 to CO and formate, but that the reaction does so at comparable or less negative potentials versus RHE relative to aqueous neutral or acidic electrolytes.

Selective electrolysis to C_1 products is tolerated in DMSO/AcOH with up to 1 M of added water

Water is an inevitable reaction product of the cathodic deoxygenation of CO_2. However, it is unclear whether having a high water content in the electrolyte would erode CO_2 reduction selectivity in favor of HER. To examine the influence of added water on the product distribution, galvanostatic electrolyses were conducted in CO_2 saturated DMSO/AcOH electrolytes with 1 M added water ("wet DMSO/ACOH"). **Figure 2a** demonstrates that a high CO selectivity (ca. 80%) can still be achieved at sufficiently negative potentials (ca. −0.73 V vs Cc/Cc^+). Its faradaic efficiency is comparable to DMSO/AcOH on the RHE scale. However, **Figure S9** demonstrates that the rate of CO formation is enhanced with the addition of water, demonstrating that the invariance in FE is not due to a corresponding invariance in CO formation rates.

Unlike in DMSO/AcOH, H_2 is observed under the tested galvanostatic range. To understand if the promotion of hydrogen originates from a change in the proton activity of the medium, **Figure 2b** depicts H_2 formation rates versus the RHE reference scale. The increase in the H_2 faradaic efficiency at aligned

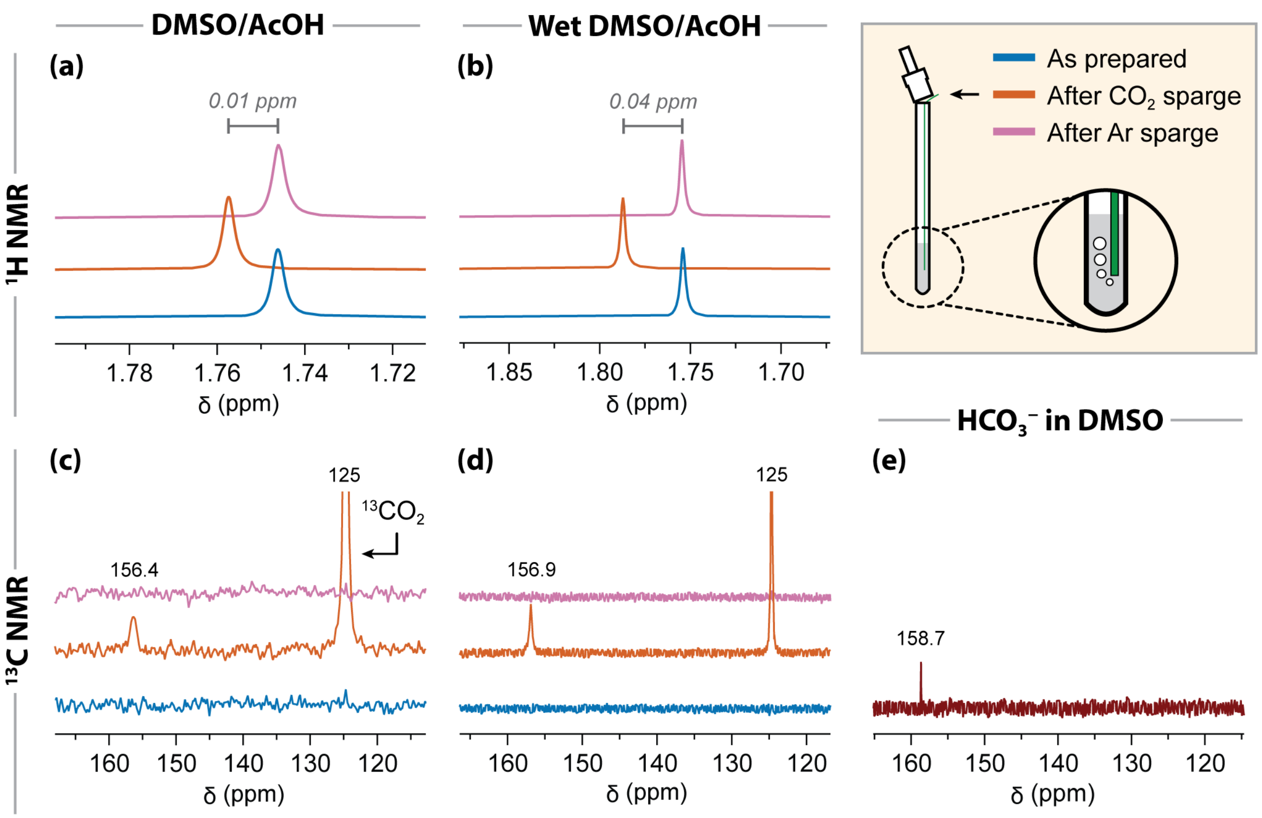

Figure 3. (a,b) ^{1}H NMR spectra depicting the acetate methyl shift in (a) DMSO/AcOH and (b) wet DMSO/AcOH electrolytes, and (c,d) ^{13}C NMR of (c) DMSO/AcOH and (d) wet DMSO/AcOH electrolyte under the following conditions: as prepared (blue), after sparging with $^{13}CO_2$ (orange), and after sparging with Ar (pink). (e) ^{13}C NMR reference spectra of tetraethylammonium bicarbonate ($TEAHCO_3^-$) in DMSO. For visual clarity, data in (c) is shown with 20 Hz exponential apodization.

potentials versus RHE in DMSO/AcOH versus wet DMSO/AcOH shows that the addition of water promotes H_2 formation. Despite this, low faradaic efficiencies for H_2 (~5%) can still be achieved with sufficiently negative applied potentials. Together, the data indicate that a high selectivity for C_1 products can still be maintained in electrolytes containing substantial amounts of added water at sufficiently negative applied potentials. Given the hygroscopic nature of DMSO, we acknowledge that sustaining operation of this system would require continuous removal of water as its produced from CO_2 deoxygenation. This could be accomplished within the cell upon development of efficient and selective catalysts for water oxidation in this medium, or can be carried out externally to the cell by, for example, membrane-based pervaporative dehydration of the electrolyte;[31,32] either approach requires substantial further development in future studies. Notwithstanding, the data implies that accumulation of water will have a negligible effect on the reaction selectivity up to the tested limit.

(Wet) DMSO/AcOH electrolyte resists electrolyte carbonation

In contrast to aqueous electrolytes, we hypothesized that electrolyte carbonation could be substantially mitigated with an AcOH/AcO$^-$ buffer in DMSO. First, we sought to understand if AcO$^-$ irreversibly forms an adduct with CO_2 via nucleophilic attack, which is one pathway for electrolyte carbonation with an exogenous donor. In order to probe a potential irreversible reaction between acetate and CO_2, ^{1}H NMR spectra were recorded on gas tight samples of DMSO/AcOH and wet DMSO/AcOH prior to and after sparging with $^{13}CO_2$ (see SI section 1.5 for experimental details). Introduction of CO_2 to the electrolyte causes a nominal change in the chemical shift of the acetate methyl resonance in both DMSO/AcOH (**Figure 3a**) and wet DMSO/AcOH (**Figure 3b**) of <0.05 ppm, evincing a weak interaction between CO_2 and AcOH/AcO$^-$ buffer. The small change chemical shift could be attributed to weak interaction between CO_2 and acetate, or a change in speciation of AcOH/AcO$^-$ buffer, or both. Regardless, subsequent sparging of the electrolyte with Ar caused the acetate methyl resonance to return to its native chemical shift, suggesting that the interaction between acetate buffer and CO_2 is indeed reversible.

Next, we sought to understand whether significant equilibrium concentrations of (bi)carbonate are formed from CO_2 hydration with water in the presence of the AcOH/AcO$^-$. Upon saturation with $^{13}CO_2$, the ^{13}C NMR spectra of DMSO/AcOH (**Figure 3c**) and wet DMSO/AcOH (**Figure 3d**) electrolyte both display a carbon signal centered at 156-157 ppm. The chemical shift of this signal is very similar to that of bicarbonate in DMSO, whose shift was independently measured to be 158.7 ppm (**Figure 3e**). Hence, we ascribe the signal primarily to the presence of equilibrium bicarbonate species. However, saturation of both electrolytes with Ar thereafter eliminates the bicarbonate resonance, implying that, unlike aqueous alkaline electrolytes, CO_2 capture is reversible in this reaction medium. Quantitative ^{13}C NMR analysis of the $^{13}CO_2$ saturated electrolyte samples revealed an equilibrium bicarbonate concentration of ca. 6 mM in DMSO/AcOH and ca. 41 mM in wet DMSO/AcOH (see SI section 1.5 for details). Both these concentrations are far below the estimated concentration of soluble

CO_2 of ca. 0.157 M in DMSO/AcOH and ca. 0.152 M in wet DMSO/AcOH. Importantly, the low equilibrium bicarbonate concentration represents a small fraction of the total anionic charge in the medium. Since the analytical concentration of acetate added to the electrolyte is 0.150 M, and since the total anion concentration must be preserved regardless of the equilibrium speciation, then bicarbonate constitutes only 4% and 27% of base-derived anionic charge. These fractions and concentrations are remarkably lower than the 100% anion carbonation at hundreds-of-millimolar quantities, with irreversible capture of CO_2, expected in alkaline aqueous electrolytes.

The low equilibrium concentration of bicarbonate in DMSO/AcOH reflects the similarity in the acidity of the AcOH/AcO$^-$ and the CO_2/HCO_3^- acid-base equilibria in DMSO. To further understand this, the pK_a of the CO_2/HCO_3^- equilibrium was estimated by calculating the proton activity differences of two independent solutions of each buffer via the equilibrium H^+/H_2 reaction on Pt (SI section 2.3 for experimental and mathematical details). We stress that this calculation is an estimate, and that a fully accurate determination of the pK_a requires explicit knowledge of all solution equilibria and any non-idealities in species' activities. Nevertheless, in acknowledging that the errors are expected to be small on a logarithmic scale, we calculate a pK_a value of 13.0 for the CO_2/HCO_3^- equilibrium. The similarity of the pK_a value of this equilibrium relative to that of AcOH/AcO$^-$ in DMSO (12.6)[27] rationalizes the observation of some carbonation occurring via equilibrium H_2CO_3 deprotonation. Despite this, our analysis demonstrates that carbonation can still be managed to millimolar levels in an aprotic solvent by, alongside reducing the water activity in the electrolyte, maintaining an electrolyte acidity close that of the CO_2/HCO_3^- acid-base equilibrium. Importantly, the similarity of the pK_a to that of AcOH/AcO$^-$ also rationalizes the observation of a high C_1 formation selectivity at negative applied potentials, similar to previous studies utilizing CO_2/HCO_3^- as the sole proton donating medium in aprotic solvents.[22]

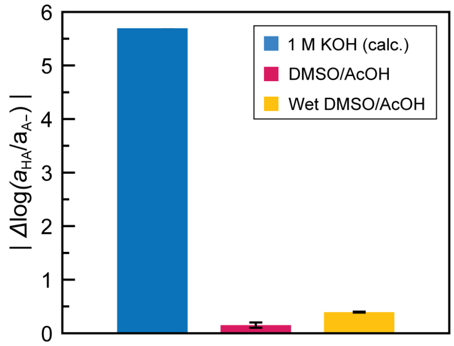

Figure 4. Difference in proton activity of DMSO/AcOH (magenta) and wet DMSO/AcOH (yellow) electrolytes before and after exposure to 0.5 atm Ar and 0.5 atm CO_2. In both conditions, 0.5 atm H_2 was present to maintain reaction equilibrium. The theoretical change to the proton activity (pH) for a 1 M solution of KOH reacting with CO_2 to form 1 M $KHCO_3$ was calculated from a previous literature report (blue).[10]

The results discussed above imply that exposure of the electrolyte to CO_2 should also not cause a significant change in the proton activity of the medium. To measure this, the equilibrium potential of the H^+/H_2 redox couple was measured under 0.5 atm partial pressure of Ar, followed by exposure to 0.5 atm partial pressure of CO_2. In both atmospheres, the H_2 partial pressure is held constant at 0.5 atm to maintain the H^+/H_2 reaction equilibrium. As seen in **Figure S10**, the equilibrium potential changes by 8 ± 3 mV in DMSO/AcOH and 23 ± 0.4 mV in wet DMSO/AcOH upon addition of CO_2. These changes in equilibrium potential translate to an effective change in proton activity of 0.14 ± 0.05 and 0.39 ± 0.01 units in DMSO/AcOH and wet DMSO/AcOH, respectively (**Figure 4**). For comparison, both changes are far less than the many-unit change in pH observed in aqueous alkaline electrolytes upon carbonation. For example, the expected equilibrium potential change in a 1 M KOH electrolyte (pH = 14) undergoing carbonation to 1 M $KHCO_3$ (pH = 8.3) is 336 mV, representing a proton activity change of more than 5.7 units (**Figure 4, Figure S10**).[10] This analysis demonstrates that the proton activity of the medium is largely unaffected by exposure to CO_2, due to its similarity in pK_a to AcOH. This result contrasts with aqueous alkaline electrolytes, where exposure to CO_2 lowers the electrolyte pH at the expense of the CO_2RR reaction selectivity.

We note that while (bi)carbonate species could be electrochemically generated at the interface, our results suggest that such species are transient. For example, previous literature has suggested that carbonate can be formed from an electroreductive disproportionation pathway between two equivalents of CO_2.[33] Recent literature has contested this observation, suggesting instead that bicarbonate formation appears because of nucleophilic attack of hydroxide on CO_2 following the direct reduction of water.[25] The foregoing data demonstrates that AcOH/AcO$^-$ drives the thermochemistry of proton transfer of the electrolyte. Hence, regardless of the pathway of its formation, electrogenerated (bi)carbonates are expected to rapidly equilibrate with AcOH/AcO$^-$ to establish the low bulk equilibrium bicarbonate concentration.

In summary, the data demonstrate that CO_2 is largely inert to DMSO/AcOH electrolytes and results in a negligible change in the proton activity of the medium upon its introduction, even with 1 M of added water. Furthermore, electrolyte carbonation can be significantly inhibited to millimolar levels by driving the thermodynamics of proton transfer and PCET with AcOH/AcO$^-$ buffer alongside attenuating the bulk water content of the electrolyte. These results contrast with CO_2RR in aqueous electrolytes, where proton donation in any pH regime comes at the cost of either low electrolyte carbonation or high CO_2RR faradaic efficiency at low overpotentials.

Conclusion

In this study, we sought to understand if selective CO_2 electroreduction catalysis could be balanced with minimal electrolyte carbonation in an aprotic electrolyte medium containing a non-nucleophilic buffer. We find that CO_2 electroreduction catalysis on pc-Au cathodes in DMSO/AcOH electrolyte affords high selectivity for C_1 products without concomitant HER at comparable potentials versus RHE relative to those previously reported in neutral aqueous electrolytes, and favorable to those in acidic aqueous electrolytes. With AcOH/AcO$^-$ buffer and an attenuated water content, we find that DMSO inhibits electrolyte carbonation to millimolar equilibrium bicarbonate concentrations. Furthermore, the proton activity of DMSO/AcOH media is largely unchanged upon CO_2 addition, demonstrating that the pK_a of CO_2/HCO_3^- is closely matched to that of AcOH/AcO$^-$. Together, our findings suggest that combining the attenuated water content in the organic media along with a non-nucleophilic buffer with a matched pK_a is an effective strategy for simultaneously mitigating carbonation and HER. We acknowledge that the practical device implementation of aprotic solvent-based CO_2RR systems is far from mature, requiring simultaneous advances in gas delivery, anode reactivity, electrolyte conductivity, water management, and cell and membrane design. However, the approach described here addresses a fundamental knowledge gap in how the activity of water, the pK_a of the proton donor, and the nucleophilicity of conjugate base can be tailored to *decouple* selective CO_2 reduction and electrolyte carbonation. By addressing this core fundamental challenge in CO_2RR, this work establishes electrolyte design principles for fostering selective fuel synthesis with minimal energy and carbon losses.

ASSOCIATED CONTENT

SUPPORTING INFORMATION

The Supporting Information is available free of charge via the Internet at [ACS website URL].

AUTHOR INFORMATION

Corresponding Author

* Yogesh Surendranath − Department of Chemistry, Massachusetts Institute of Technology, Cambridge, Massachusetts 02139, United States; orcid.org/0000-0003-1016-3420; Email: yogi@mit.edu

Authors

An T. Chu – Department of Chemistry, Massachusetts Institute of Technology, Cambridge, Massachusetts 02139, United States; orcid.org/0000-0002-7259-6005

Onyu Jung – Department of Chemistry, Massachusetts Institute of Technology, Cambridge, Massachusetts 02139, United States

Wei Lun Toh – Department of Chemistry, Massachusetts Institute of Technology, Cambridge, Massachusetts 02139, United States; https://orcid.org/0000-0001-9001-0488

Notes

The authors declare no competing financial interest.

ACKNOWLEDGMENT

This work was supported primarily by the Air Force Office of Scientific Research (AFOSR) under award number FA95502010291. A.T.C. graciously acknowledges Max Hüelsey for experimental assistance and the Surendranath Lab for their support and scientific discussions. This work was carried out in part through the use of MIT.nano's facilities.

REFERENCES

(1) Overa, S.; Ko, B. H.; Zhao, Y.; Jiao, F. Electrochemical Approaches for CO_2 Conversion to Chemicals: A Journey toward Practical Applications. *Acc. Chem. Res.* **2022**, *55* (5), 638–648.

(2) Shih, C. F.; Zhang, T.; Li, J.; Bai, C. Powering the Future with Liquid Sunshine. *Joule* **2018**, *2* (10), 1925–1949.

(3) Nitopi, S.; Bertheussen, E.; Scott, S. B.; Liu, X.; Engstfeld, A. K.; Horch, S.; Seger, B.; Stephens, I. E. L.; Chan, K.; Hahn, C.; Nørskov, J. K.; Jaramillo, T. F.; Chorkendorff, I. Progress and Perspectives of Electrochemical CO2 Reduction on Copper in Aqueous Electrolyte. *Chem. Rev.* **2019**, *119* (12), 7610–7672.

(4) Hall, A. S.; Yoon, Y.; Wuttig, A.; Surendranath, Y. Mesostructure-Induced Selectivity in CO2 Reduction Catalysis. *J. Am. Chem. Soc.* **2015**, *137* (47), 14834–14837.

(5) Wuttig, A.; Yaguchi, M.; Motobayashi, K.; Osawa, M.; Surendranath, Y. Inhibited Proton Transfer Enhances Au-Catalyzed CO_2-to-Fuels Selectivity. *Proc. Natl. Acad. Sci.* **2016**, *113* (32).

(6) Yoon, Y.; Hall, A. S.; Surendranath, Y. Tuning of Silver Catalyst Mesostructure Promotes Selective Carbon Dioxide Conversion into Fuels. *Angew. Chemie Int. Ed.* **2016**, *55* (49), 15282–15286.

(7) Raciti, D.; Mao, M.; Park, J. H.; Wang, C. Local PH Effect in the CO2 Reduction Reaction on High-Surface-Area Copper Electrocatalysts. *J. Electrochem. Soc.* **2018**, *165* (10), F799–F804.

(8) Lu, X.; Zhu, C.; Wu, Z.; Xuan, J.; Francisco, J. S.; Wang, H. In Situ Observation of the PH Gradient near the Gas Diffusion Electrode of CO_2 Reduction in Alkaline Electrolyte. *J. Am. Chem. Soc.* **2020**, *142* (36), 15438–15444.

(9) Rabinowitz, J. A.; Kanan, M. W. The Future of Low-Temperature Carbon Dioxide Electrolysis Depends on Solving One Basic Problem. *Nat. Commun.* **2020**, *11* (1), 5231.

(10) Ma, M.; Clark, E. L.; Therkildsen, K. T.; Dalsgaard, S.; Chorkendorff, I.; Seger, B. Insights into the Carbon Balance for CO_2 Electroreduction on Cu Using Gas Diffusion Electrode Reactor Designs. *Energy Environ. Sci.* **2020**, *13* (3), 977–985.

(11) Dunwell, M.; Lu, Q.; Heyes, J. M.; Rosen, J.; Chen, J. G.; Yan, Y.; Jiao, F.; Xu, B. The Central Role of Bicarbonate in the Electrochemical Reduction of Carbon Dioxide on Gold. *J. Am. Chem. Soc.* **2017**, *139* (10), 3774–3783.

(12) Wuttig, A.; Yoon, Y.; Ryu, J.; Surendranath, Y. Bicarbonate Is Not a General Acid in Au-Catalyzed CO 2 Electroreduction. *J. Am. Chem. Soc.* **2017**, *139* (47), 17109–17113.

(13) Hori, Y. Electrochemical CO2 Reduction on Metal Electrodes. In *Modern Aspects of Electrochemistry*; Springer New York: New York, NY; pp 89–189.

(14) Huang, J. E.; Li, F.; Ozden, A.; Sedighian Rasouli, A.; García de Arquer, F. P.; Liu, S.; Zhang, S.; Luo, M.; Wang, X.; Lum, Y.; Xu, Y.; Bertens, K.; Miao, R. K.; Dinh, C.-T.; Sinton, D.; Sargent, E. H. CO_2 Electrolysis to Multicarbon Products in Strong Acid. *Science (80-.).* **2021**, *372* (6546), 1074–1078.

(15) O'Brien, C. P.; Miao, R. K.; Liu, S.; Xu, Y.; Lee, G.; Robb, A.; Huang, J. E.; Xie, K.; Bertens, K.; Gabardo, C. M.; Edwards, J. P.; Dinh, C.-T.; Sargent, E. H.; Sinton, D. Single Pass CO_2

Conversion Exceeding 85% in the Electrosynthesis of Multicarbon Products via Local CO_2 Regeneration. *ACS Energy Lett.* **2021**, *6* (8), 2952–2959.

(16) Pan, B.; Fan, J.; Zhang, J.; Luo, Y.; Shen, C.; Wang, C.; Wang, Y.; Li, Y. Close to 90% Single-Pass Conversion Efficiency for CO_2 Electroreduction in an Acid-Fed Membrane Electrode Assembly. *ACS Energy Lett.* **2022**, *7* (12), 4224–4231.

(17) Xie, K.; Miao, R. K.; Ozden, A.; Liu, S.; Chen, Z.; Dinh, C.-T.; Huang, J. E.; Xu, Q.; Gabardo, C. M.; Lee, G.; Edwards, J. P.; O'Brien, C. P.; Boettcher, S. W.; Sinton, D.; Sargent, E. H. Bipolar Membrane Electrolyzers Enable High Single-Pass CO_2 Electroreduction to Multicarbon Products. *Nat. Commun.* **2022**, *13* (1), 3609.

(18) Gu, J.; Liu, S.; Ni, W.; Ren, W.; Haussener, S.; Hu, X. Modulating Electric Field Distribution by Alkali Cations for CO_2 Electroreduction in Strongly Acidic Medium. *Nat. Catal.* **2022**, *5* (4), 268–276.

(19) García de Arquer, F. P.; Dinh, C.-T.; Ozden, A.; Wicks, J.; McCallum, C.; Kirmani, A. R.; Nam, D.-H.; Gabardo, C.; Seifitokaldani, A.; Wang, X.; Li, Y. C.; Li, F.; Edwards, J.; Richter, L. J.; Thorpe, S. J.; Sinton, D.; Sargent, E. H. CO2 Electrolysis to Multicarbon Products at Activities Greater than 1 A Cm−2. *Science (80-.).* **2020**, *367* (6478), 661–666.

(20) König, M.; Vaes, J.; Klemm, E.; Pant, D. Solvents and Supporting Electrolytes in the Electrocatalytic Reduction of CO_2. *iScience* **2019**, *19*, 135–160.

(21) Joshi, P. B.; Karki, N.; Wilson, A. J. Electrocatalytic CO_2 Reduction in Acetonitrile Enhanced by the Local Environment and Mass Transport of H2O. *ACS Energy Lett.* **2022**, *7* (2), 602–609.

(22) Haynes, L. V.; Sawyer, D. T. Electrochemistry of Carbon Dioxide in Dimethyl Sulfoxide at Gold and Mercury Electrodes. *Anal. Chem.* **1967**, *39* (3), 332–338.

(23) Ito, K.; Ikeda, S.; Yamauchi, N.; Iida, T.; Takagi, T. Electrochemical Reduction Products of Carbon Dioxide at Some Metallic Electrodes in Nonaqueous Electrolytes. *Bull. Chem. Soc. Jpn.* **1985**, *58* (10), 3027–3028.

(24) Shi, J.; Shen, F.; Shi, F.; Song, N.; Jia, Y.-J.; Hu, Y.-Q.; Li, Q.-Y.; Liu, J.; Chen, T.-Y.; Dai, Y.-N. Electrochemical Reduction of CO_2 into CO in Tetrabutylammonium Perchlorate/Propylene Carbonate: Water Effects and Mechanism. *Electrochim. Acta* **2017**, *240*, 114–121.

(25) Figueiredo, M. C.; Ledezma-Yanez, I.; Koper, M. T. M. In Situ Spectroscopic Study of CO_2 Electroreduction at Copper Electrodes in Acetonitrile. *ACS Catal.* **2016**, *6* (4), 2382–2392.

(26) Vijh, A. K.; Conway, B. E. Electrode Kinetic Aspects of the Kolbe Reaction. *Chem. Rev.* **1967**, *67* (6), 623–664.

(27) Izutsu, K. *Electrochemistry in Nonaqueous Solutions*; Wiley, 2009.

(28) Roberts, J. A. S.; Bullock, R. M. Direct Determination of Equilibrium Potentials for Hydrogen Oxidation/Production by Open Circuit Potential Measurements in Acetonitrile. *Inorg. Chem.* **2013**, *52* (7), 3823–3835.

(29) Chu, A. T.; Surendranath, Y. Aprotic Solvent Exposes an Altered Mechanism for Copper-Catalyzed Ethylene Electrosynthesis. *J. Am. Chem. Soc.* **2022**, *144* (12), 5359–5365.

(30) Ringe, S.; Morales-Guio, C. G.; Chen, L. D.; Fields, M.; Jaramillo, T. F.; Hahn, C.; Chan, K. Double Layer Charging Driven Carbon Dioxide Adsorption Limits the Rate of Electrochemical Carbon Dioxide Reduction on Gold. *Nat. Commun.* **2020**, *11* (1), 33.

(31) Zhang, Y.; Chong, J. Y.; Xu, R.; Wang, R. Effective Separation of Water-DMSO through Solvent Resistant Membrane Distillation (SR-MD). *Water Res.* **2021**, *197*, 117103.

(32) Hasegawa, Y.; Abe, C.; Ikeda, A. Pervaporative Dehydration of Organic Solvents Using High-Silica CHA-Type Zeolite Membrane. *Membranes (Basel).* **2021**, *11* (3), 229.

(33) Amatore, C.; Saveant, J. M. Mechanism and Kinetic Characteristics of the Electrochemical Reduction of Carbon Dioxide in Media of Low Proton Availability. *J. Am. Chem. Soc.* **1981**, *103* (17), 5021–5023.

For TOC

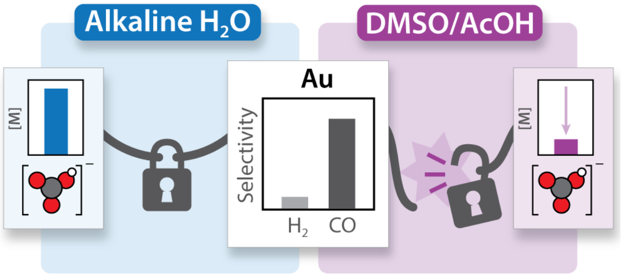

Attenuating electrolyte carbonation and decoupling it from electrolyte acidity during selective CO_2RR